RSC Advances

PAPER

View Article Online
View Journal | View Issue

Cite this: *RSC Adv.*, 2015, **5**, 35753

Assembly of hybrids based on polyoxotungstates and Co-tris(imidazolyl) complexes with bifunctional electrocatalytic activities†

Wanli Zhou,[ab] Jun Peng,*[a] Zheyu Zhang,[a] Zhenyu Shi,[a] Shifa Ullah Khan[a] and Hongsheng Liu*[c]

Received 20th January 2015
Accepted 13th April 2015

DOI: 10.1039/c5ra01165e

www.rsc.org/advances

Three new organic–inorganic hybrid compounds based on the Keggin polyoxometalates, $[Co_2(tib)_2(H_2O)_4(\alpha\text{-}HBW_{12}O_{40})]\cdot 6H_2O$ (**1**), $[Co_2(tib)_2(H_2O)_4(\alpha\text{-}SiW_{12}O_{40})]\cdot 4H_2O$ (**2**) and $[Co(H_2tib)_4(\alpha\text{-}BW_{12}O_{40})_2]\cdot 8H_2O$ (**3**) (tib = 1,3,5-tris(1-imidazoly)benzene), were hydrothermally synthesized by utilizing a pH-dependent approach in the same POM/Co/tib reaction systems. X-ray structural analyses reveal that isostructural compounds **1** and **2**, obtained at pH 3.6, have a (3,4)-connected 2D net with the (4^2 6)(4^2 6^3 8) topology; compound **3**, isolated at pH 4.8, is a "butterfly-like" structure stemming from α-BW_{12} polyoxoanions and Co–tib motifs. In addition, the electrocatalytic properties of compounds **1–3** were studied by cyclic voltammetry. Compounds **1–3** displayed bifunctional electrocatalytic activities toward reduction of nitrite and oxidation of ascorbic acid.

Introduction

Polyoxometalates (POMs) have been extensively used in crystal engineering during the past decades to build organic–inorganic hybrid complexes because of their structural diversity and versatile applications in areas such as magnetism, catalysis, electrochemistry, gas storage/separation, and so on.[1,2] The Keggin POMs are important members in the POM family, which have abundant of surface oxygen atoms, acting as either coordination atoms to modify metal ions in multiple modes, or hydrogen bonding acceptors in many cases to confirm the frameworks. An effective strategy to build POM-based hybrid materials is to make use of the Keggin POMs and d-block metal complexes coordinated by N-heterocycle ligands as building units, to acquire multiple dimension organic–inorganic hybrid frameworks by using hydrothermal technique.[3] Among the d-block elements, Ag and Cu, with flexible coordination modes, have been extensively explored.[4] Co also is an important transition metal because of its extensive applications in catalysis and biological systems.[5] Generally, Co(II) ions are involved in the POM chemistry either as a central heteroatom or as multiple-nuclear cobalt clusters (from $\{Co\}_2$ to $\{Co\}_{14}$).[6] Whereas, Co complexes, as basic building blocks, were not extensively involved in the POM chemistry yet. A limited number of the Keggin POM-based hybrids containing Co–N-heterocycle complexes have been reported till now,[7] and some of them are enumerated here: $[Co_2(H_2O)(bimb)_4](HBW_{12}O_{40})\cdot H_2O$ (bimb = 1,3-bis(1-imidazoly)benzene), $[Co(bpy)_2(H_2O)]_2[SiMo_{12}V_2O_{42}]$, $[Co_2(L)_5(H_2O)_2(SiW_{12}O_{40})]$ (L = 4,4′-bis((1H-1,2,4-triazol-1-yl)-methyl)biphenyl), $K[Co(phen)_2(H_2O)]_2[HCoW_{12}O_{40}]\cdot 2H_2O$, $[Co(bpy)_3]_6(H_2bpy)[(Cobpy)_2(PMo_8Mo_4O_{40})]_3$,$\{[Co(phen)_2]_2[PMo_{12}O_{40}(VO)_2]\}\{[Co(phen)_2(OH)]_2[PMo_{12}O_{40}(VO)_2]\}\cdot 2.5H_2O$, $[(Co(bpy)(PMo_8Mo_4O_{40})]\cdot 16H_2O$, $[Co(H_2O)_2(bimb)_2[SiW_{12}O_{40}]$, and $[Co(bpy)_3]_{1.5}\{[Co(bpy)_2(H_2O)][HCoW_{12}O_{40}]\}\cdot 0.5H_2O$ (see Scheme 1). Among the N-heterocycle organic ligands, the Y-

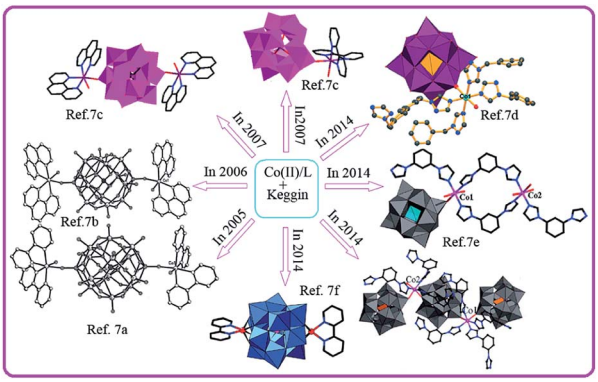

Scheme 1 A series of Keggin POM-based hybrids containing Co–N-heterocycle complexes reported in different years.

[a]*Key Laboratory of Polyoxometalate Science of Ministry of Education, Faculty of Chemistry, Northeast Normal University, Changchun, Jilin, 130024, PR China. E-mail: jpeng@nenu.edu.cn; hsliu899@126.com*

[b]*Faculty of Chemistry, Tonghua Normal University, Tonghua, Jilin, 134002, PR China*

[c]*School of Chemistry and Chemical Engineering, Daqing Normal University, Daqing, Heilongjiang, 163712, PR China*

† Electronic supplementary information (ESI) available: Selected bond lengths (Å) and angles (°) for compounds **1–3**; hydrogen bonds (Å and °) for compound **3**; figures of IR, TG, PXRD analysis. CCDC 1035487, 1035488 and 1035489. For ESI and crystallographic data in CIF or other electronic format see DOI: 10.1039/c5ra01165e

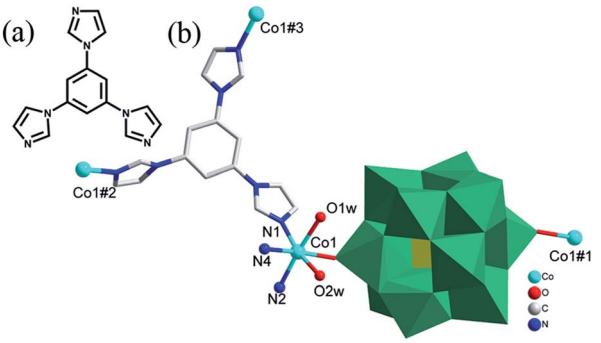

Fig. 1 (a) The tib ligand; (b) ball/stick/polyhedral view of the asymmetric unit of compound **1**. Hydrogen atoms and crystallization water molecules are omitted for clarity. Symmetry operation: #1 $1-x, 1-y, 1-z$; #2 $2-x, -1-y, 2-z$; #3 $1+x, y, z$.

shaped N-heterocycle molecule 1,3,5-tris(1-imidazoly)benzene (abbreviated as tib) is special. This molecule acting as a ligand has three features (see Fig. 1a): (i) three imidazole rings in tib can provide different coordination number and mode; (ii) the three aloof N-donors in imidazole rings will reduce steric hindrance in coordination; (iii) the tib molecule, as a rigid bridging ligand, usually exhibits μ_1, μ_2 and/or μ_3 coordination modes, and the uncoordinated N can provide N–H···O hydrogen bonding interactions between POMs and metal–tib complex groups. Therefore, we select the Keggin POMs and Co–tib complex groups as building blocks to assemble POM-based hybrid materials. In our POM/Co/tib reaction systems, pH is a crucial factor to influence the hybrid assembly. Herein, we report three new compounds, $[Co_2(tib)_2(H_2O)_4(\alpha\text{-}HBW_{12}O_{40})]\cdot 6H_2O$ (**1**), $[Co_2(tib)_2(H_2O)_4(\alpha\text{-}SiW_{12}O_{40})]\cdot 4H_2O$ (**2**) and $[Co(H_2tib)_4(\alpha\text{-}BW_{12}O_{40})_2]\cdot 8H_2O$ (**3**), which were obtained in different pH conditions by hydrothermal method. Electrocatalytic properties for compounds **1–3** have also been investigated.

Experimental

Chemicals and instruments

All the chemicals purchased were of reagent grade and used without further purification. $K_7Na[\alpha\text{-}HBW_{11}O_{39}]\cdot 13H_2O$ and $K_8[\alpha\text{-}SiW_{11}O_{39}]\cdot 13H_2O$ were prepared according to the literature method,[8] and verified by IR spectra. Element analyses for Co, B, Si and W were performed on a Leeman inductivity-coupled plasma (ICP) spectrometer, while the elemental analyses for C, H and N were performed on a Perkin-Elmer 2400 elemental analyzer. IR spectra were recorded on an ExoScan FTIR spectrometer with KBr pellets in the 400–4000 cm^{-1} region. Thermogravimetric (TG) analyses were carried out on a Diamond thermogravimetric analyzer in N_2 atmosphere from 50 °C to 1000 °C at a heating rate of 10 °C min^{-1}. Power XRD diffractograms were recorded on a Bruker D8X diffractometer equipped with monochromatized Cu-Kα ($\lambda = 1.5418$ Å) radiation in the range of $5 \leq 2\theta \leq 50$, with a scanning rate of 4° s^{-1}. Cyclic voltammograms were obtained with a CHI-604E electrochemical workstation at room temperature, with a platinum wire as the counter electrode, a Ag/AgCl electrode as the reference electrode, and the carbon paste electrodes (CPE) modified with compounds **1–3** (**1**-, **2**- and **3**-CPE) as working electrodes.

X-ray crystallography

Selected single crystals of compounds **1–3** were fixed onto thin glass fibers by epoxy glue in air for data collection. Diffraction data were collected on a Bruker Apex II CCD with Mo-Kα radiation ($\lambda = 0.71073$ Å). An empirical absorption correction was applied. All the structures were solved by the directed method and refined by full-matrix least-squares on F^2. All calculations were performed using the SHELX-97 program package.[9] All the non-hydrogen atoms were anisotropically refined. Details of the X-ray structural analyses for compounds **1–3** are given in Table 1, and the selected bond lengths and angles are listed in Tables S1–S3.†

Syntheses of compounds 1–3

$[Co_2(tib)_2(H_2O)_4(\alpha\text{-}HBW_{12}O_{40})]\cdot 6H_2O$ (1). A mixture of $K_7Na[\alpha\text{-}HBW_{11}O_{39}]\cdot 13H_2O$ (abbreviated as $\alpha\text{-}BW_{11}$) (0.3025 g), $Co(NO_3)_2\cdot 6H_2O$ (0.1068 g) and tib (0.0428 g) was dissolved in 7 mL of distilled water, and stirred for 0.5 h. The resulted suspension was kept in a 25 mL-Teflon-lined autoclave after its pH value was adjusted to 3.6 with 3 M acetic acid, and heated at 433 K for six days. Then the autoclave was slowly cooled to room temperature, and yellow block crystals were harvested by filtration, dried in air (0.0568 g; yield, 23.5%, based on W). Elemental analyses for $C_{30}H_{45}O_{50}N_{12}Co_2BW_{12}$ found (Calcd) (%): B 0.30 (0.32), W 60.35 (60.30), Co 3.13 (3.10), C 9.69 (9.65), H 1.21 (1.20), N 4.49 (4.45). IR (cm^{-1}): 2916 (s), 2848 (s), 1555 (w), 1463 (s), 1379 (w), 1269 (w), 1090 (w), 1031 (s), 727 (s), 718 (s), 664 (w).

$[Co_2(tib)_2(H_2O)_4(\alpha\text{-}SiW_{12}O_{40})]\cdot 4H_2O$ (2). Compound **2** was prepared following the procedure described for compound **1**, but $K_8[\alpha\text{-}SiW_{11}O_{39}]\cdot 13H_2O$ (abbreviated as $\alpha\text{-}SiW_{11}$) was used instead of $\alpha\text{-}BW_{11}$. Red block crystals were obtained after six days (0.0638 g; yield, 31.6%, based on W). Elemental analyses for $C_{30}H_{40}O_{48}N_{12}Co_2SiW_{12}$ found (Calcd) (%): Si 0.75 (0.80), W 60.65 (60.75), Co 3.18 (3.20), C 9.72 (9.70), H 0.11 (0.10), N 4.54 (4.50). IR (cm^{-1}): 3120 (s), 2850 (s), 1641 (m), 1460 (m), 1359 (m), 1090 (s), 952 (m), 880 (s), 729 (s), 650 (w).

$[Co(H_2tib)_4(\alpha\text{-}BW_{12}O_{40})_2]\cdot 8H_2O$ (3). Compound **3** was prepared following the procedure described for compound **1**, except that the pH value was adjusted to 4.8 with 3 M acetic acid. Red block crystals were obtained after six days (0.0526 g, yield, 20.6%, based on W). Elemental analyses for $C_{60}H_{72}O_{88}N_{24}CoB_2W_{24}$ found (Calcd) (%): B 0.32 (0.28), W 60.85 (60.95), Co 0.84 (0.80), C 10.28 (10.35), H 0.12 (0.15), N 4.79 (4.75). IR (cm^{-1}): 3550 (s), 2100 (w), 1627 (w), 1520 (m), 950 (s), 837 (s), 799 (w), 718 (s), 664 (m).

Preparations of *n*-CPE (n = 1–3)

The *n*-CPE (n = **1–3**) was prepared as follows: 10 mg of compound n and 90 mg of graphite powder were mixed, and ground together to homogeneous, into which 0.2 mL of paraffinic oil was added with stirring. The such-obtained paste was

Table 1 Crystal data and structure refinement for compounds **1–3**

Compound reference	**1**	**2**	**3**
Chemical formula	$C_{30}H_{45}O_{50}N_{12}Co_2BW_{12}$	$C_{30}H_{40}O_{48}N_{12}Co_2SiW_{12}$	$C_{60}H_{72}O_{88}N_{24}CoB_2W_{24}$
FW	3708.65	3688.89	7030.37
Crystal system	Triclinic	Triclinic	Triclinic
a/Å	11.730(5)	11.706(5)	12.300(5)
b/Å	12.368(5)	12.743(5)	13.241(5)
c/Å	13.453(5)	13.415(5)	18.837(5)
α/°	70.126(5)	70.234(5)	98.227(5)
β/°	67.298(5)	67.789(5)	94.896(5)
γ/°	64.847(5)	65.151(5)	93.212(5)
V/Å^3	1635.7(11)	1642.4(11)	3018.0(19)
Temperature/K	293(2)	293(2)	293(2)
Space group	$P\bar{1}$	$P\bar{1}$	$P\bar{1}$
Z	1	1	1
μ/mm^{-1}	21.609	21.536	23.012
F(000)	1656	1644	3117
Final $R_1{}^a$, w$R_2{}^b$ ($I > 2\sigma(I)$)	0.0824, 0.1806	0.0798, 0.1696	0.0505, 0.1248
Final $R_1{}^a$, w$R_2{}^b$ (F^2) (all data)	0.0920, 0.1849	0.0975, 0.1787	0.0753, 0.1544
Goodness of fit on F^2	1.039	1.069	1.061

^{a} $R_1 = \sum||F_o| - |F_c||/\sum|F_o|$. ^{b} w$R_2 = [\sum w(F_o^2 - F_c^2)^2/\sum w(F_o^2)^2]^{1/2}$.

packed into a glass tube with 2.0 mm inner diameter, and the surface was wiped with paper. The electrical contact was established with a copper rod through the back of the electrode.

Results and discussion

Structural descriptions of compounds 1–3

Single-crystal X-ray diffraction analyses indicate that compounds **1** and **2** are isostructural, and crystallized in the triclinic space group $P\bar{1}$. Here only the structure of compound **1** is described in details. The basic structural unit of compound **1** is composed of one α-BW_{12} polyanion, an isolated Co^{2+} ion, one tib ligand and five water molecules (Fig. 1b). The α-BW_{12} polyanion exhibits a classic Keggin structure, consisting of a central $\{BO_4\}$ tetrahedron and four vertex-sharing M_3O_{13} groups, and each M_3O_{13} cluster is composed of three $\{WO_6\}$ octahedra linked in a triangular arrangement by sharing edges. The W–O (1.694–2.484 Å) and B–O (1.444–1.603 Å) bond distances are in the reasonable ranges,[10] and the central four μ_4-O atoms are disordered over eight positions with each oxygen site half-occupied, a common phenomenon for the Keggin POM clusters.[11]

The Co1 atom is six-coordinated in an octahedral geometry, defined by three N atoms (N1, N4 and N5) from three tib ligands, one terminal O atom (O1) of the α-BW_{12} cluster, and two coordination water molecules (O1w and O2w) (Fig. 2a). The bond lengths of Co–O (2.096 Å to 2.17) and Co–N (2.11 Å to 2.16 Å) are in the reasonable ranges.[7] The α-BW_{12} polyoxoanion acts as a bidentate ligand to link two Co^{II} ions. The bond valence sum calculations[12] indicate that all the tungsten atoms are in the +VI oxidation state, and cobalt atoms in the +II oxidation state. To balance the charge of the compound, a proton is needed, then compound **1** is formulated as $[Co_2(tib)_2(H_2O)_4(\alpha\text{-}HBW_{12}O_{40})]\cdot 6H_2O$.

The structural feature of compound **1** is the 2D network constructed from circle-connecting-circle Co–tib chains bridging α-BW_{12} polyanions. Each Co–tib chain is formed by diamond $\{Co_2(tib)_2\}$ circles, which are connected together through sharing the imidazole rings in each $\{Co_2(tib)_2\}$ circle (*ca.* 11.0 Å × 5.6 Å), and the $\{Co_2(tib)_2\}$ circles fold in pairs to form a wave-like chain (Fig. 2b). The α-BW_{12} anion, acting as a two-connected inorganic ligand, offers two terminal oxygen atoms (O1) to coordinate with Co1. Finally, the neighbouring chains are connected by μ_2-O (O1) of α-BW_{12} polyanion to create a net framework along the c-axis (Fig. 2c). From the topology point of view, tib ligands and Co1 atoms as three- and four-connected nodes, respectively, thus the whole structure can be rationalized as a (3,4)-connected 2D network with the (4^2 6)(4^2 6^3 8) topology (Fig. 2d). The dissociative water molecules are inserted among the 2D sheets, extending the net frameworks to a 3D supramolecule structure through hydrogen bonding.

Compound **3** consists of α-BW_{12} clusters and $[Co(H_2tib)_4]^{10+}$ motifs with "butterfly-like" structure, and crystallizes in the triclinic space group $P\bar{1}$. As shown in Fig. 3, the asymmetric unit

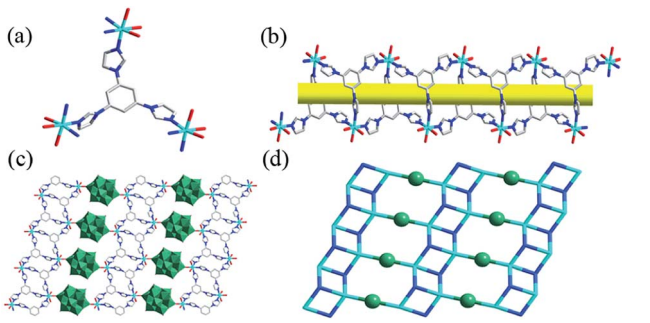

Fig. 2 Ball/stick/polyhedral views of (a) the coordination mode of tib; (b) the chain formed by Co^{II} ions and tib ligands; (c) 2D net composed of circle-connecting-circle Co–tib chains through sharing POMs; (d) topology of the 2D network, in compound **1**. Color code: BW_{12} polyoxoanion, sea green; Co^{II} ion, turquoise; tib, light blue.

of compound **3** contains a Co^{2+} ion, four tib ligands, two inverse Keggin α-BW_{12} polyanions and four water molecules. Bond valence sum calculations indicate that all the tungsten atoms are in the +VI oxidation state, B atom in the +III oxidation, and cobalt atoms in the +II oxidation state. Compound **3** is formulated as $[Co_2(H_2tib)_4(\alpha\text{-}BW_{12}O_{40})]\cdot 8H_2O$, in which two protons are added to balance the charge of the compound. In the unit cell, Co1 atom is six-coordinated in an octahedral geometry by two bridging oxygen atoms (O2, O2#) from two α-BW_{12} and four N donors (N5, N5#, N7, N7#) from four tib ligands, respectively.

Each tib ligand coordinates to Co1 ion in a μ_1-N–Co (N5 or N7) bonding mode, with other two N sites protonated. In this way, four tib ligands coordinate to Co1, forming a "butterfly"-type $Co(tib)_4$ group. The bond distances of B–O vary from 1.502 Å to 1.552 Å, and the angles of O–B–O are between 108.3(14)° and 110.4°, close to tetrahedral 109.28°. The Co–O distances are 2.173(13) Å, and the Co–N distances are in the range from 2.090(16) Å to 2.142(18) Å. The angles of O–Co–O are 180°, and the angles of N–Co–N are in the range from 86.6(17) to 180°, which are comparable with those found in other reported cobalt compounds.[7] The N–H···O distances are between 1.747 and 2.568 Å. The dissociative water molecules link the POM clusters and the "butterfly-like" $Co(tib)_4$ groups in hydrogen bonding to generate a 3D supramolecular structure (Fig. 4). The hydrogen bonds are listed in Table S4.†

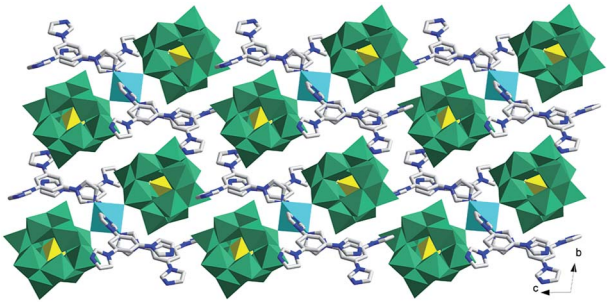

Fig. 4 View of the 3D supramolecular structure for compound **3**.

Influence of pH on the final structures in the POMs, Co and tib hydrothermal reaction system

Generally, hydrothermal reaction systems are regarded as a black box, in which many factors can affect reaction mechanisms and conformations of final products. In this work, compounds **1–3** were obtained under the same hydrothermal reaction system with merely different pH: the original pH is 3.6 for compounds **1** and **2**, 4.8 for compound **3** (Fig. 5). When original pH was below 3.6 or above 5.2, no crystalline products were formed. The influence of pH on this system perhaps in the following aspects: (i) the species of the Keggin POMs are pH-dependent.[13] In the range of pH 3.6–5.2, the superior species of the Keggin POMs is the saturate one, rather than the lacunary one. Resultantly, the starting material α-XW_{11} transfers to α-XW_{12}, and the freshly generated XW_{12} species exhibits more active to coordinate to the metals. (ii) The reactions need lower pH to avoid the deposition of cobalt hydroxide. (iii) Coordination mode of tib ligand is affected by pH due to different protonation of the N atoms. In compounds **1–3**, tib molecules exhibit μ_1-and μ_3-coordination modes.

FT-IR spectra, TG analyses and powder X-ray diffraction (PXRD)

IR spectra of compounds **1–3** are shown in Fig. S1.† The absorbance bands in the region of 720–990 cm^{-1} are ascribed to the characteristic vibrations of the $\nu_{as}(W\text{–}O_d)$, $\nu_{as}(X\text{–}O_a)$, $\nu_{as}(W\text{–}O_b\text{–}W)$ and $\nu_{as}(W\text{–}O_c\text{–}W)$ in the Keggin POMs. The sharp peaks in the region of 1000–3300 cm^{-1} are ascribed to the vibrations of the tib molecules.

TG curves of **1–3** show roughly two steps of weight-loss. The total weight-loss of *ca.* 20.0% in the range of 300–700 °C corresponds to the loss of the water molecules and tib molecules, in detail, 20.0% (calculated 19.7%) for compound **1**, 19.0% (calculated 18.7%) for compound **2** and 18.0% (calculated 17.7%) for compound **3** (Fig. S2–S4†).

Purities of compounds **1–3** were checked by PXRD comparisons of the samples with simulation of single-crystal XRD data.

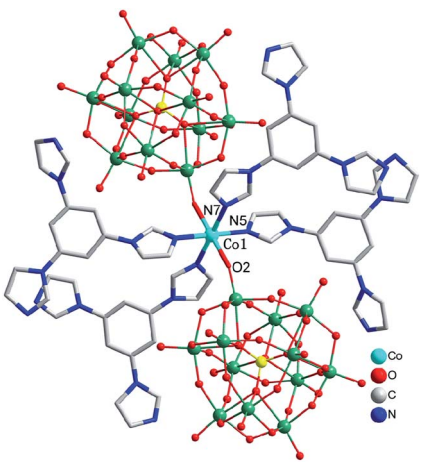

Fig. 3 Ball/stick view of the asymmetric unit of compound **3**. Hydrogen atoms and water molecules are omitted for clarity.

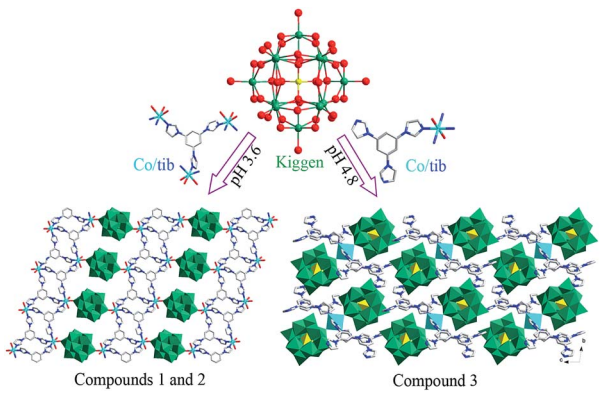

Fig. 5 Illustration of the structural features for compounds **1–3** generated in different pH media.

The experimental and simulated XRD patterns of compounds **1–3** are consistent (Fig. S5†), which demonstrates that the phase purities of the products are good.

Electrochemical and electrocatalytic properties

Electrochemical properties of compounds **1–3** were investigated in a 1 M H_2SO_4 + Na_2SO_4 aqueous solution (pH = 1) through CV measurements with *n*-CPE (*n* = **1–3**) in the potential range from +500 to −1000 mV at a scan rate of 0.02 V s^{-1}. As the redox processes of α-SiW_{12} and α-BW_{12} POMs have been well defined by POM chemists,[14] for comparison, CV measurements with CPEs made of corresponding potassium salts (α-SiW_{12}-CPE and α-BW_{12}-CPE) were also made under the same conditions. The cyclic voltammograms are shown in Fig. 6. The cyclic voltammograms of α-SiW_{12}-CPE and α-BW_{12}-CPE are comparable to corresponding CVs of *n*-CPE, which are helpful to assign the cyclic voltammograms. The midpoint potentials (E_m) of the redox couples I–I′, II–II′ and III–III′, estimated by using the two tangent method, are 0.14, −0.40 and −0.80 V for **1**-CPE; −0.18, −0.43 and −0.62 V for **2**-CPE; −0.03, −0.42 and −0.63 V for **3**-CPE.

The couple I–I′ is ascribed to the redox process of Co^{III}/Co^{II} centre,[7e] and the couples II–II′ and III–III′ can be ascribed to two one-electron redox processes of W^{VI}/W^{V} centres for *n*-CPE (*n* = **1** and **3**).[15] Whereas, the couples I–I′, II–II′ and III–III′ for **2**-CPE are ascribed to two reversible one-electron waves followed by a reversible two-electron wave occurring in the W^{VI}/W^{V} centres, respectively,[16] and it is noticed that the redox wave of Co^{III}/Co^{II} centre is not obvious.

Electrocatalysis is an important application in the POM chemistry due to POMs' rich redox properties. Nitrite and ascorbic acid (AA) are usually used as probes of electrocatalytic redox reactions in electrocatalytic studies.[7e,17] In this work, electrocatalytic properties of compounds **1–3** are investigated through CV measurements with *n*-CPE (*n* = **1–3**) in the presences of nitrite and AA in 1 M H_2SO_4 + Na_2SO_4 aqueous solutions (pH = 1), respectively (Fig. 7 and 8).

In Fig. 7, obvious increase of the reduction peak currents (II′ and III′) along with the increase of nitrite concentration is observed; meanwhile the corresponding oxidation peak currents keep basically unchanged, indicating that II′ and III′ cathodic waves of XW_{12} (X = Si or B) possess good electrocatalytic activity for nitrite reduction. It is known that NO_2^- disproportionates to form NO and NO_3^- in acid solutions.[18] We deduce that the reduction mechanism involves reductions of NO_2^- and NO by the heteropoly blue species (eqn (1) and (2) in ESI†).

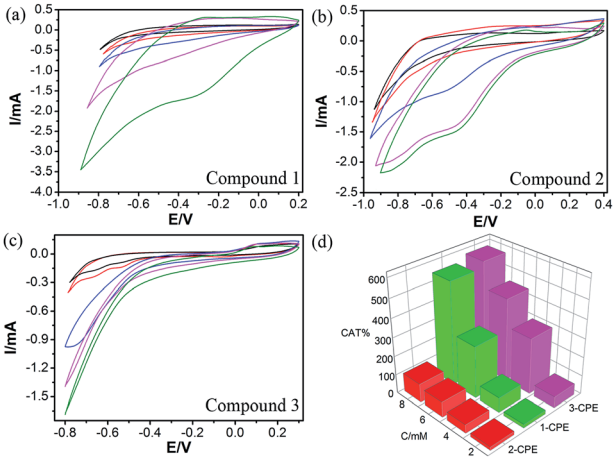

Fig. 7 Cyclic voltammograms showing the electrocatalytic oxidation of NO_2^- by (a) **1**-CPE, (b) **2**-CPE and (c) **3**-CPE in 1 M H_2SO_4 + Na_2SO_4 solutions (pH = 1) with increase of concentration of AA, from up to bottom: 0, 2 × 10^{-3}, 4 × 10^{-3}, 6 × 10^{-3}, 8 × 10^{-3} mol L^{-1}. Scan rate: 0.1 V s^{-1}. (d) Chart of CAT% *vs.* concentration of AA for *n*-CPE (*n* = **1–3**).

In Fig. 8, significant increase of the oxidation peak currents of Co^{II} along with the increase of AA concentration is observed. The oxidation reactions of ascorbic acid are electrocatalyzed obviously by the couple of Co^{III}/Co^{II}. The proposed oxidation mechanism is shown in eqn (3) in ESI.†[19]

The electrocatalytic efficiency (CAT) of *n*-CPE (*n* = **1–3**) are calculated by adopting the CAT formula:[20]

$$\mathrm{CAT} = 100\% \times [I_p\,(\mathrm{C, substrate}) - I_p\,(\mathrm{C})]/I_p\,(\mathrm{POM})$$

where I_p (C, substrate) is the current intensity of a catalytic wave for an electro-catalyst in the presence of substrate, and I_p (C) is the current intensity of the catalyst in the absence of substrate. Here CAT% are calculated according to the current intensities of cathodic wave III' in the presence of substrate (NO_2^-), and the current intensities of anodic wave of couple Co^{III}/Co^{II} in the presence of substrate (AA) for *n*-CPE (*n* = **1–3**). Histograms of CAT% for *n*-CPE (*n* = **1–3**) *vs.* concentrations of substrate are

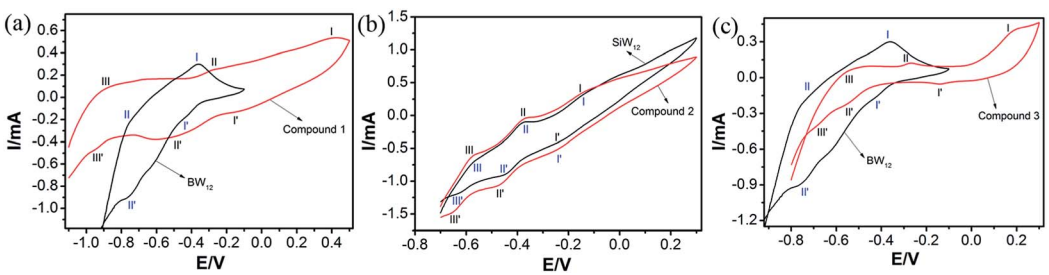

Fig. 6 The cyclic voltammograms of *n*-CPE (*n* = **1–3**) (red line) with comparisons to those of α-BW_{12}-CPE and α-SiW_{12}-CPE (black line) in 1 M H_2SO_4 + Na_2SO_4 solutions at a scan rate of 0.02 V s^{-1}.

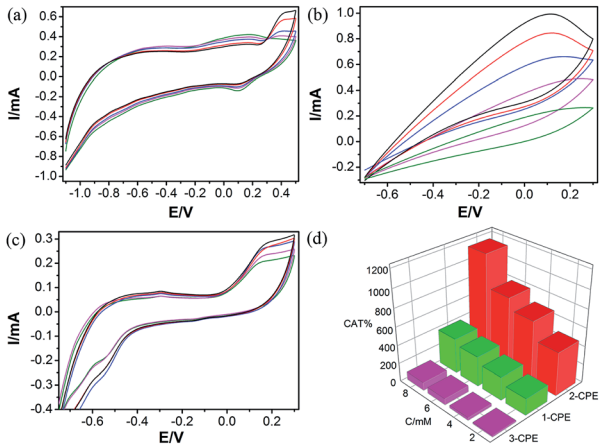

Fig. 8 Cyclic voltammograms showing the electrocatalytic reduction of AA by (a) **1**-CPE, (b) **2**-CPE and (c) **3**-CPE in 1 M H_2SO_4 + Na_2SO_4 solutions (pH = 1) with increase of concentration of NO_2^-, from up to bottom: 0, 2×10^{-3}, 4×10^{-3}, 6×10^{-3}, 8×10^{-3} mol L^{-1}. Scan rate: 0.1 V s^{-1}. (d) Chart of CAT% *vs.* concentration of NO_2^- for *n*-CPE (*n* = **1–3**).

shown in Fig. 7d and 8d for intuitive comparisons of the electrocatalytic activities (Table S5†).

The electrocatalytic efficiencies of *n*-CPE are in an order of **3**-CPE > **1**-CPE > **2**-CPE for nitrite reduction, and **2**-CPE > **1**-CPE > **3**-CPE for AA oxidation. These results indicate that Keggin α-BW_{12} hybrids exhibit better performances than that for Keggin α-SiW_{12} hybrid towards electrocatalytic reduction of NO_2^-, and conversely, Keggin α-SiW_{12} hybrid exhibits a better performance towards electrocatalytic oxidations of AA than those for Keggin α-BW_{12} hybrids. The differences of electrocatalytic performances between the two series of Keggin POM hybrids and between α-BW_{12} hybrids should be due to the differences in their structures and electrochemical properties.

Furthermore, the stability of *n*-CPE have been investigated by repeating 40 cycles of the electrocatalytic nitrite reduction with a single carbon paste electrode in 1 M H_2SO_4 + Na_2SO_4 solution, and the CVs are shown in Fig. S6.† The CVs remain almost unchanged after 40 cycles. This fact indicates that these compounds are stable, and electrocatalytic activity towards reduction of nitrite is maintained during the repeating catalytic experiments.

In summary, compounds **1–3** possess bifunctional electrocatalytic activities towards reduction of nitrite ascribed to the W-center and oxidation of ascorbic acid ascribed to the Co-centre.

Conclusions

We have obtained three new organic–inorganic hybrid compounds based on Keggin POMs and Co–tib units under identical hydrothermal conditions but in different pH media. Compounds **1** and **2** were obtained at pH 3.6, which exhibited an isostructural (3,4)-connected 2D framework with the $(4^2\,6)(4^2\,6^3\,8)$ topology. With increase of pH to 4.8, compound **3** was isolated, which had a "butterfly-like" structure stemmed from α-BW_{12} polyoxoanions and Co–tib motifs. The structural differences of compounds **1–3** indicate that pH is a vital factor for the assembly in the hydrothermal reaction system of Keggin POMs, Co(II) ions and tib ligands. Furthermore, electrochemical and electro-catalytic properties of compounds **1–3** were investigated in 1 M Na_2SO_4 + H_2SO_4 media through CV measurements. The CV experiments show that compounds **1–3** have bifunctional electrocatalytic activities toward not only reduction of NO_2^- but also oxidation of biologic molecule AA. We are extending this work to other organic and inorganic ligands to synthesize POM/Co/L hybrid compounds with novel architectures and prominent properties.

Acknowledgements

We thank the National Natural Science Foundation of China (Grant 21373044 and 21171030) for financial supports.

Notes and references

1 (*a*) M. T. Pope and A. Müller, *Angew. Chem., Int. Ed.*, 1991, **30**, 34; (*b*) D. L. Long, E. Burkholder and L. Cronin, *Chem. Soc. Rev.*, 2007, **36**, 105; (*c*) U. Kortz, A. Müller, J. V. Slageren, J. Schnack, N. S. Dalal and M. Dressel, *Coord. Chem. Rev.*, 2009, **253**, 2315; (*d*) L. Cronin and A. Muller, *Chem. Soc. Rev.*, 2012, **41**, 7333; (*e*) H. N. Miras, C. J. Richmond, D. L. Long and L. Cronin, *J. Am. Chem. Soc.*, 2012, **134**, 3816; (*f*) N. V. Izarova, M. T. Pope and U. Kortz, *Angew. Chem., Int. Ed.*, 2012, **51**, 9492; (*g*) U. Kortz and T. Liu, *Eur. J. Inorg. Chem.*, 2013, 1559; (*h*) C. H. Zhan, J. W. Cameron, J. Gao, J. M. Purcell, D. L. Long and L. Cronin, *Angew. Chem., Int. Ed.*, 2014, **53**, 1; (*i*) W. M. Xuan, A. J. Surman, H. N. Miras, D. L. Long and L. Cronin, *J. Am. Chem. Soc.*, 2014, **136**, 14114.

2 (*a*) S. T. Zheng, J. Zhang and G. Y. Yang, *Angew. Chem., Int. Ed.*, 2008, **47**, 3909; (*b*) G. Gao, F. Li, L. Xu, X. Liu and Y. Yang, *J. Am. Chem. Soc.*, 2008, **130**, 10838; (*c*) S. G. Mitchell, C. Streb, H. N. Miras, T. Boyd, D. L. Long and L. Cronin, *Nat. Chem.*, 2010, **2**, 308; (*d*) D. L. Long, R. Tsunashima and L. Cronin, *Angew. Chem., Int. Ed.*, 2010, **49**, 1736; (*e*) F. J. Ma, S. X. Liu, C. Y. Sun, D. D. Liang, G. J. Ren, F. Wei, Y. G. Chen and Z. M. Su, *J. Am. Chem. Soc.*, 2011, **133**, 4178; (*f*) P. Huang, C. Qin, Z. M. Su, Y. Xing, X. L. Wang, K. Z. Shao, Y. Q. Lan and E. B. Wang, *J. Am. Chem. Soc.*, 2012, **134**, 14004; (*g*) A. M. Khenkin, I. Efremenko, J. M. L. Martin and R. Neumann, *J. Am. Chem. Soc.*, 2013, **135**, 19304; (*h*) D. Y. Du, J. S. Qin, S. L. Li, Z. M. Su and Y. Q. Lan, *Chem. Soc. Rev.*, 2014, **43**, 4615.

3 (*a*) Y. P. Ren, X. J. Kong, X. Y. Hu, M. Sun, L. S. Long, R. B. Huang and L. S. Zheng, *Inorg. Chem.*, 2006, **45**, 4016; (*b*) J. Q. Sha, J. Peng, H. S. Liu, J. Chen, B. X. Dong, A. X. Tian and Z. M. Su, *Eur. J. Inorg. Chem.*, 2007, 1268; (*c*) X. L. Wang, H. L. Hu and A. X. Tian, *Cryst. Growth Des.*, 2010, **10**, 4786; (*d*) X. L. Wang, J. Li, A. X. Tian, D. Zhao, G. C. Liu and H. Y. Lin, *Cryst. Growth Des.*, 2011, **11**, 3456; (*e*) X. L. Wang, Q. Gao, A. X. Tian and G. C. Liu, *Cryst.*

Growth Des., 2012, **12**, 2346; (*f*) M. G. Liu, P. P. Zhang, J. Peng, H. X. Meng, X. Wang, M. Zhu, D. D. Wang, C. L. Meng and K. Alimaje, *Cryst. Growth Des.*, 2012, **12**, 1273; (*g*) M. T. Li, J. Q. Sha, X. M. Zong, J. W. Sun, P. F. Yan, L. Li and X. N. Yang, *Cryst. Growth Des.*, 2014, **14**, 2794; (*h*) A. X. Tian, Y. Yang, J. Ying, N. Li, X. L. Lin, J. W. Zhang and X. L. Wang, *Dalton Trans.*, 2014, 8405; (*i*) X. L. Wang, N. Li, A. X. Tian, J. Ying, T. J. Li, X. L. Lin, J. Luan and Y. Yang, *Inorg. Chem.*, 2014, **53**, 7118.

4 (*a*) J. Q. Sha, J. Peng, S. J. Zhou, M. Zhu, L. Han and D. Chen, *J. Cluster Sci.*, 2008, **19**, 499; (*b*) Y. H. Luo, X. Y. Yu and H. Zhang, *CrystEngComm*, 2014, **16**, 6664; (*c*) X. Y. Wu, Q. K. Zhang, X. F. Kuang, W. B. Yang, R. M. Yu and C. Z. Lu, *Dalton Trans.*, 2012, 11783; (*d*) C. Zhang, X. Lin, Z. Zhang, L. S. Long, C. Wang and W. Lin, *Chem. Commun.*, 2014, **50**, 11591.

5 (*a*) A. Taleb, C. Petit and M. P. Pileni, *J. Phys. Chem. B*, 1998, **102**, 2214; (*b*) X. Liu, G. C. Guo, M. L. Fu, X. H. Liu, M. S. Wang and J. S. Huang, *Inorg. Chem.*, 2006, **45**, 3679; (*c*) C. N. Lok, C. M. Ho, R. Chen, Q. Y. He, W. Y. Yu, H. Z. Sun, P. K. Tam, J. F. Chiu and C. M. Che, *J. Proteome Res.*, 2006, **5**, 916; (*d*) A. Panacek, L. Kvıtek, R. Prucek, M. Kolar, R. Vecerova, N. Pizurova, V. K. Sharma, T. Neveca and R. Zboril, *J. Phys. Chem. B*, 2006, **110**, 16248; (*e*) S. Okamoto and L. D. Eltis, *Metallomics*, 2011, **3**, 963; (*f*) D. Lindsay and W. Kerr, *Nat. Chem.*, 2011, **3**, 494.

6 (*a*) M. D. Ritorto, T. M. Anderson, W. A. Neiwert and C. L. Hill, *Inorg. Chem.*, 2004, **43**, 44; (*b*) J. M. Clemente-Juan, E. Coronado, A. Forment-Aliaga, J. R. Galán-Mascarüs, C. Giménez-Saiz and C. J. Gómez-García, *Inorg. Chem.*, 2004, **43**, 2689; (*c*) C. Lydon, M. M. Sabi, M. D. Symes, D. L. Long, M. Murrie, S. Yoshii, H. Nojiri and L. Cronin, *Chem. Commun.*, 2012, **48**, 9819; (*d*) J. Gao, J. Yan, S. Beeg, D. L. Long and L. Cronin, *J. Am. Chem. Soc.*, 2013, **135**, 1796; (*e*) J. W. Vickers, H. J. Lv, J. M. Sumliner, G. B. Zhu, Z. Luo, D. G. Musaev, Y. V. Geletii and C. L. Hill, *J. Am. Chem. Soc.*, 2013, **135**, 14110; (*f*) H. Lv, J. Song, Y. V. Geletii, W. Guo, J. Bacsa and C. L. Hill, *Eur. J. Inorg. Chem.*, 2013, 1720; (*g*) J. Guo, D. Zhang, L. Chen, Y. Song, D. Zhu and Y. Xu, *Dalton Trans.*, 2013, 8454; (*h*) M. Ibrahim, A. Haider, Y. H. Lan, B. S. Bassil, A. M. Carey, R. J. Liu, G. J. Zhang, B. Keita, W. H. Li, G. E. Kostakis, A. K. Powell and U. Kortz, *Inorg. Chem.*, 2014, **53**, 5179; (*i*) X. B. Han, Z. M. Zhang, T. Zhang, Y. G. Li, W. B. Lin, W. S. You, Z. M. Su and E. B. Wang, *J. Am. Chem. Soc.*, 2014, **136**, 5359.

7 (*a*) Z. Y. Shi, X. J. Gu, J. Peng and Y. H. Chen, *J. Solid State Chem.*, 2005, **178**, 1988; (*b*) Z. Y. Shi, J. Peng, C. J. Gómez-García, S. Benmansour and X. J. Gu, *J. Solid State Chem.*, 2006, **179**, 253; (*c*) J. Q. Sha, J. Peng, J. Chen, H. S. Liu, A. X. Tian and P. P. Zhang, *Solid State Sci.*, 2007, **9**, 1012; (*d*) Y. H. Luo, X. Y. Yu and H. Zhang, *CrystEngComm*, 2014, **16**, 6664; (*e*) T. T. Yu, K. Wang, H. Y. Ma, H. J. Pang and S. B. Li, *RSC Adv.*, 2014, **4**, 2235; (*f*) C. Zhang, X. Lin, Z. Zhang, L. S. Long, C. Wang and W. Lin, *Chem. Commun.*, 2014, **50**, 11591.

8 (*a*) N. Haraguchi, Y. Okaue and T. Isobe, *Inorg. Chem.*, 1994, **33**, 1015; (*b*) A. Téazéa, G. Hervéa and G. R. Finke, *Inorg. Synth.*, 1990, **27**, 85.

9 (*a*) G. M. Sheldrick, *SHELXS-97*, Program for solution of crystal structures, University of Göottingen, Germany, 1997; (*b*) G. M. Sheldrick, *SHELXL-97*, Program for refinement of crystal structures, University of Göottingen, Germany, 1997.

10 (*a*) H. Y. An, E. B. Wang, D. R. Xiao, Y. G. Li, Z. M. Su and L. Xu, *Angew. Chem., Int. Ed.*, 2006, **45**, 904; (*b*) H. Y. An, Z. B. Han and T. Q. Xu, *Inorg. Chem.*, 2010, **49**, 11403; (*c*) X. Wang, M. M. Zhang, X. L. Hao, Y. H. Wang, Y. Wei, F. S. Liang, L. J. Xu and Y. G. Li, *Cryst. Growth Des.*, 2013, **13**, 3454.

11 H. T. Evans and M. T. Pope, *Inorg. Chem.*, 1984, **23**, 501.

12 (*a*) I. D. Brown and D. Altermatt, *Acta Crystallogr., Sect. B: Struct. Sci.*, 1985, **41**, 244; (*b*) A. Trzesowska, R. Kruszynski and J. T. Bartczak, *Acta Crystallogr., Sect. B: Struct. Sci.*, 2004, **60**, 174; (*c*) N. E. Brese and M. O. Keefe, *Acta Crystallogr., Sect. B: Struct. Sci.*, 1991, **47**, 192.

13 (*a*) A. R. Oliva, V. Sans, H. N. Miras, J. Yan, H. Y. Zang, C. J. Richmond, D. L. Long and L. Cronin, *Angew. Chem., Int. Ed.*, 2012, **51**, 12759; (*b*) W. L. Zhou, Z. Y. Zhang, J. Peng, X. Wang, Z. Y. Shi and G. Z. Li, *CrystEngComm*, 2014, **16**, 10893.

14 (*a*) N. L. Laronze, J. Marrot, G. Herve, R. Thourenot and E. Cadot, *Chem.–Eur. J.*, 2007, **13**, 7234; (*b*) Y. Shen, J. Peng, H. Q. Zhang, X. Yu and A. M. Bond, *Inorg. Chem.*, 2012, **51**, 5146.

15 A. Teze, M. Michelon and G. Herve, *Inorg. Chem.*, 1997, **36**, 505.

16 M. Sadakane and E. Steckhan, *Chem. Rev.*, 1998, **98**, 219.

17 (*a*) S. Dong, X. Xi and M. Tian, *J. Electroanal. Chem.*, 1995, **385**, 227; (*b*) J. E. Toth and F. C. Anson, *J. Electroanal. Chem.*, 1988, **256**, 361; (*c*) X. L. Wang, H. Zhang, E. B. Wang, Z. B. Han and C. W. Hu, *Mater. Lett.*, 2004, **58**, 661.

18 F. A. Cotton and G. Wilkinson, *Advanced Inorganic Chemistry*, Wiley, New York, 1988, p. 327.

19 (*a*) P. Wang, X. P. Wang, X. Y. Jing and G. Y. Zhu, *Anal. Chim. Acta*, 2000, **424**, 51; (*b*) C. Sun and J. Zhang, *Electrochim. Acta*, 1998, **43**, 943; (*c*) Y. Shen, J. Peng, H. J. Pang, P. P. Zhang, D. Chen, C. Y. Chen, H. Q. Zhang, C. L. Meng and Z. M. Su, *Chem.–Eur. J.*, 2011, **17**, 3657.

20 (*a*) B. Keita, A. Belhouari, L. Nadjo and R. J. Contant, *Electroanal. Chem.*, 1995, **381**, 243; (*b*) B. X. Dong, J. Peng, A. X. Tian, J. Q. Sha, L. Li and H. S. Liu, *Electrochim. Acta*, 2007, **52**, 3804; (*c*) H. Zhang, K. Yu, C. M. Wang, Z. H. Su, C. X. Wang, D. Sun, H. H. Cai, Z. Y. Chen and B. B. Zhou, *Inorg. Chem.*, 2014, **53**, 12337.